BIOCHEMISTRY
including biophysical chemistry & molecular biology

Article

pubs.acs.org/biochemistry

Effect of Exchange of the Cysteine Molybdenum Ligand with Selenocysteine on the Structure and Function of the Active Site in Human Sulfite Oxidase

Stefan Reschke,[†] Dimitri Niks,[‡] Heather Wilson,[§] Kajsa G. V. Sigfridsson,[∥,⊥] Michael Haumann,[∥] K. V. Rajagopalan,[§] Russ Hille,[‡] and Silke Leimkühler*,[†]

[†]Department of Molecular Enzymology, Institute of Biochemistry and Biology, University of Potsdam, 14476 Potsdam, Germany

[‡]Department of Biochemistry, University of California, Riverside, California 92521, United States

[§]Department of Biochemistry, Duke University Medical Center, Durham, North Carolina 27710, United States

[∥]Institute of Experimental Physics, Free University Berlin, 14195 Berlin, Germany

Supporting Information

ABSTRACT: Sulfite oxidase (SO) is an essential molybdoenzyme for humans, catalyzing the final step in the degradation of sulfur-containing amino acids and lipids, which is the oxidation of sulfite to sulfate. The catalytic site of SO consists of a molybdenum ion bound to the dithiolene sulfurs of one molybdopterin (MPT) molecule, carrying two oxygen ligands, and is further coordinated by the thiol sulfur of a conserved cysteine residue. We have exchanged four non-active site cysteines in the molybdenum cofactor (Moco) binding domain of human SO (SOMD) with serine using site-directed mutagenesis. This facilitated the specific replacement of the active site Cys207 with selenocysteine during protein expression in *Escherichia coli*. The sulfite oxidizing activity (k_{cat}/K_M) of $SeSOMD_{4Ser}$ was increased at least 1.5-fold, and the pH optimum was shifted to a more acidic value compared to those of $SOMD_{4Ser}$ and $SOMD_{4Cys(wt)}$. X-ray absorption spectroscopy revealed a Mo^{VI}−Se bond length of 2.51 Å, likely caused by the specific binding of Sec207 to the molybdenum, and otherwise rather similar square-pyramidal $S/Se(Cys)O_2Mo^{VI}S_2(MPT)$ site structures in the three constructs. The low-pH form of the Mo(V) electron paramagnetic resonance (EPR) signal of $SeSOMD_{4Ser}$ was altered compared to those of $SOMD_{4Ser}$ and $SOMD_{4Cys(wt)}$, with g_1 in particular shifted to a lower magnetic field, due to the Se ligation at the molybdenum. In contrast, the Mo(V) EPR signal of the high-pH form was unchanged. The substantially stronger effect of substituting selenocysteine for cysteine at low pH as compared to high pH is most likely due to the decreased covalency of the Mo−Se bond.

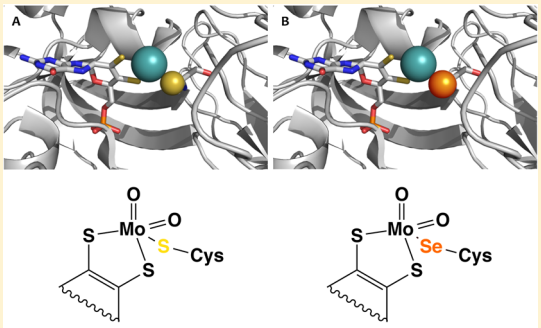

Molybdenum enzymes containing the molybdenum cofactor (Moco) are ubiquitous in biology and perform essential reactions, including degradation of amino acids, nucleotides, and various drugs.[1] The Moco enzymes have been categorized into three groups, two of which are present in mammals, namely, the xanthine oxidase (XO) and sulfite oxidase (SO) families.[2] Mammalian SO (EC 1.8.3.1) is an essential enzyme that resides in the intermembrane space of mitochondria and is responsible for the oxidation of sulfite to sulfate, which is the final reaction in the degradation of sulfur-containing compounds, including the amino acids methionine and cysteine.[3] SO deficiency, due to a mutation either in the respective gene or in the genes responsible for Moco biosynthesis, leads to severe neurological problems that often result in death at an early age.[4,5]

Mammalian SO is a homodimer with a subunit mass of ∼51 kDa. Each monomer contains an N-terminal domain binding a cytochrome b_5 ($cytb_5$) heme, a C-terminal domain containing the molybdenum ligated to the dithiolene sulfurs of one molybdopterin (MPT) molecule, and in addition a dimerization domain.[3] The N- and C-terminal domains of each subunit are linked by a flexible hinge region. The two-electron oxidation of sulfite to sulfate is known to occur at the molybdenum site, which is reduced from Mo(VI) to Mo(IV), followed by intramolecular electron transfer to the $cytb_5$ site, with cytochrome *c* serving as the terminal electron acceptor.[6] The movement of domains between the Moco domain and the $cytb_5$ domain facilitated by the flexible linker is essential for efficient electron transfer between the heme and the Moco.[7] In addition, the SO Moco binding domain (SOMD) has the ability to oxidize sulfite in the presence of artificial electron acceptors like ferricyanide.[8]

In the crystal structure of chicken liver SO, the molybdenum atom is pentacoordinated in a square pyramidal geometry, with three sulfur and two terminal oxygen ligands.[3] Two of the sulfur

Received: July 1, 2013
Revised: October 16, 2013
Published: October 22, 2013

dx.doi.org/10.1021/bi4008512 | *Biochemistry* 2013, 52, 8295−8303

atoms are from the dithiolene group of MPT, and the third is from the thiol side chain of Cys185 (Cys207 in human SO). The dithiolene sulfurs of MPT also are involved in the transfer of the oxo group from water to the sulfite molecule during catalysis.[6] The importance of the Cys207 residue has been demonstrated by site-directed mutagenesis and EPR studies of human SO in which Cys207 was replaced with serine.[9] The amino acid exchange resulted in a trioxomolybdenum center with strongly reduced activity.[10] Charge density maps of chicken liver SO have suggested that electrons may be sequentially transferred out of the molybdenum center, following docking of the heme domain at the surface of the substrate access channel.[11] It has been proposed that Cys185, which is directed toward this channel, may act as an electron transfer relay between Mo and the *b*-type heme.[6]

To clarify the role of Cys207 for substrate oxidation and electron transfer, we have replaced it with a selenocysteine by providing selenocysteine substituting for sulfur sources during protein expression. The ionic radii and electronegativities of selenium and sulfur are similar, but selenide is a stronger reducing agent than sulfide. Because of the lower p*K* values of selenols compared with those of thiols, selenocysteine tends to be deprotonated under physiological conditions, whereas cysteine tends to be protonated.[12] Several molybdenum- and tungsten-containing enzymes have been shown to contain selenium either as a selenocysteine ligand to the Mo site, e.g., in formate dehydrogenases,[13] or as an inorganic selenium ligand to the Mo site, e.g., in selected enzymes of the XO family.[14] In both cases, replacement of Se with S was found to decrease the catalytic activity of the enzymes.[15]

In this study, we have compared the catalytic activity and spectroscopic properties of wild-type human SOMD, containing four non-active site cysteine residues and the active site Cys207 [$SOMD_{4Cys(wt)}$], with those of constructs in which only the four cysteines were changed to serine ($SOMD_{4Ser}$) or, in addition, Cys207 was replaced with Sec207 ($SeSOMD_{4Ser}$). In the SOMD construct, the cytb_5 domain of the SO was deleted so that the usual intramolecular electron transfer from the Moco to cytb_5 did not occur and an exogenously added electron acceptor could be used instead. This facilitated EPR studies specifically of the Mo(V) site. Enzyme kinetic investigations in addition to XAS and EPR results revealed the binding of Sec207 to the Mo atom, and the impact of the substitution on the activity, coordination environment, and protonation properties of the active site.

MATERIALS AND METHODS

Bacterial Strains, Plasmids, Growth Conditions, and Protein Purification. The amino acid exchanges of Cys242, Cys253, Cys260, and Cys451 for serine were introduced into plasmid pTG818[8] containing the human SOMD by using the Transformer site-directed mutagenesis kit (Invitrogen). The correct base pair exchanges were confirmed by DNA sequencing. In this construct, amino acids 1−107 containing the cytb_5 domain of the SO were deleted. *Escherichia coli* TP1000 cells containing expression vectors pTG818 and pTG818-4CysSer were grown aerobically in LB medium at 30 °C in the presence of 150 mg/L ampicillin and 20 μM IPTG for 24 h. For selenium incorporation, bacterial strains containing expression vector pTG818-4CysSer were grown aerobically in phosphate-buffered, sulfate-free M9 minimal medium (pH 7.4) first in the presence of L-cysteine. Additionally, the medium contained a 0.1% trace element solution (400 μM H_3BO_3, 30 μM $CoCl_2$, 10 μM $CuCl_2$, 10 μM $ZnCl_2$, 80 μM $MnCl_2$, and 10 mM $FeCl_3$), 0.8% glycerol, a 100 mg/L mixture of all amino acids, 1 mM $MgCl_2$, 0.5 mM $CaCl_2$, 12.6 mg/L KNO_3, and 0.3% glucose.[16]

The cultures were grown at 30 °C in the presence of 150 mg/L ampicillin to an OD_{600} of 0.8−1.2. Expression was induced with 20 μM IPTG for 15 min.[8] Cells where harvested and washed twice with sulfate-free M9 minimal medium. The cell yield of 1 L of culture was transferred to 1 L of the sulfate-free M9 medium in which cysteine was replaced with 30 mg/L selenocystine (obtained from Acros Organics, Geel, Belgium) The cultures were further grown aerobically for 24 h at 30 °C in the presence of 150 mg/L ampicillin, 20 μM IPTG, and 1 mM sodium molybdate.

Cells were harvested, and the cell pellet was resuspended in phosphate buffer [50 mM NaH_2PO_4 and 300 mM NaCl (pH 8.0)]. Cell lysis was achieved after two passes through a TS Series Benchtop cell disruptor at 1350 bar in the presence of DNase I (1 μg/mL). The cleared lysate was applied to 0.75 mL of nickel-nitrilotriacetic acid (Ni-NTA) per liter of culture. The column was washed with 20 column volumes of phosphate buffer containing sequentially 10 and 20 mM imidazole. Proteins were eluted with phosphate buffer containing 250 mM imidazole, dialyzed against 100 mM Tris (pH 7.2), and stored at −80 °C until further use. The purity of the proteins was analyzed by sodium dodecyl sulfate−polyacrylamide gel electrophoresis (SDS−PAGE).[17]

Metal Quantification by ICP-OES. Metal content analysis was performed using an Optima 2100DV inductively coupled plasma-optical emission (ICP-OES) spectrometer (Perkin-Elmer, Fremont, CA). Protein samples were incubated overnight in a 1:1 mixture with 65% nitric acid (Suprapur, Merck, Darmstadt, Germany) at 100 °C. Protein samples were diluted with a 10-fold volume of ultrapure water (Millipore) prior to ICP-OES analysis. The multielement standard solution XVI (Merck) was used as a reference.[18]

Enzyme Activity Assay. SO activity was assayed at room temperature by monitoring the reduction of the ferricyanide ion, at 420 nm in solution using a Shimadzu UV-2401 spectrophotometer. The sodium sulfite concentration was varied between 1.25 and 500 μM, and the ferricyanide concentration was kept constant at 100 μM in 50 mM Tris and 0.1 mM EDTA. For measurements at pH 6.0, phosphate citrate buffer (McIlloaine) was used.

X-ray Absorption Spectroscopy (XAS). XAS at the Mo K-edge was conducted at the SAMBA beamline of SOLEIL (Paris, France) using a Si[220] double-crystal monochromator as previously described.[19] A 36-element energy-resolving Ge detector (Canberra) was used for detection of the X-ray fluorescence of Mo, which was shielded by a 10 μm Zr foil against scattered X-rays. Samples were held in a liquid helium cryostat at 20 K. A Mo foil measured simultaneously in transmission mode was used as an energy standard (reference energy of 20003.9 eV). Data were evaluated using previously established routines and in-house software,[20] and FEFF 7[21] was used for calculation of phase functions for EXAFS (extended X-ray absorption fine structure) fit analysis. The shown XANES (X-ray absorption near-edge structure) and EXAFS spectra represent the average of three to five monochromator scans (one or two scans per sample spot). Radiation damage or X-ray photoreduction of the samples was absent, as judged from the unchanged Mo K-edge shape and energy for consecutive EXAFS scans on a single sample spot (not shown). The pre-

dx.doi.org/10.1021/bi4008512 | *Biochemistry* 2013, 52, 8295−8303

edge region of XANES spectra was isolated using XANDA [K. V. Klementiev, XANES dactyloscope for Windows (www.cells.es/Beamlines/CLAESS/software/xanda.html)].

EPR Experiments. Adjustment of the pH and H_2O-D_2O exchange in protein samples for EPR were accomplished by dilution of the concentrated protein with appropriate buffers (100 mM Tris-acetate at various pH values in H_2O or D_2O) and reconcentration thereafter. Samples were made anaerobic by being degassed at 4 °C (5−7 °C for deuterated samples) and transferred to argon-flushed, septum-sealed EPR tubes. An anaerobic solution of sodium sulfite was added to a final concentration of 2 mM for protein reduction; samples were subsequently reoxidized by one electron equivalent with either ferricyanide or O_2-saturated buffer and then rapidly frozen in an ethanol/dry ice bath before being transferred to liquid nitrogen. EPR spectra were recorded in a Bruker ST 4102 X-band cavity using a Bruker ER 300 spectrometer equipped with an ER 035 M gaussmeter and an HP 5352B microwave frequency counter. The temperature was controlled using a Bruker ER 4111 VT variable-temperature unit and a liquid nitrogen cryostat. Spectra were collected at 150 K using a microwave power of 4.0 mW and a modulation amplitude of 0.4 mT. The shown spectra represent the average of 25−100 magnetic field separate scans and were aligned to a microwave frequency of 9.4577 GHz. EPR simulations were performed using EasySpin version 3.1.0;[22] no attempt was made to simulate the contributions of ^{95}Mo and ^{97}Mo to the spectra. Signal intensities were quantified by double integration of the baseline-corrected EPR spectra using EWWIN version 6.1.

RESULTS

Expression and Purification of Human SOMD with a Selenocysteine at the Active Site. A strategy was developed for the incorporation of a selenocysteine instead of a cysteine at position 207 in the active site of the molybdenum domain of human SO (SOMD). A construct of wild-type SOMD [$SOMD_{4Cys(wt)}$] was generated, in which its four non-active site cysteines (Cys242, Cys253, Cys260, and Cys451) were replaced with serine using site-directed mutagenesis, yielding the $SOMD_{4Ser}$ construct. In this construct, the cytb_5 domain of the SO was deleted, facilitating specific spectroscopic investigations exclusively of the Moco binding site. $SOMD_{4Ser}$ was expressed as an N-terminal fusion to a His_6 tag and purified by Ni-NTA chromatography as previously described.[8] The minimal growth medium contained selenocystine instead of cysteine, which was expected to result in the incorporation of Sec207 at the active site to yield the $SeSOMD_{4Ser}$ protein.

The UV−vis absorption spectra of $SOMD_{4Cys(wt)}$ and $SOMD_{4Ser}$ were rather similar, in particular in showing significant absorbance at 350 nm, which reflects contributions to the spectra from the Moco[8] (Figure 1). In the spectrum of $SeSOMD_{4Ser}$, the magnitude of the 350 nm absorption was diminished, presumably because of a lower level of saturation of the protein with Moco (see below). However, the overall shape of the spectrum of $SeSOMD_{4Ser}$ was similar to that of $SOMD_{4Ser}$, suggesting that the amino acid environment of the Moco in both proteins remained intact. The similar spectra also suggested that Sec207 may be a ligand to the molybdenum atom in $SeSOMD_{4Ser}$, because in the absence of the Cys ligand, i.e., in the Cys207Ser mutant, a pronouncedly altered Moco spectrum has been observed previously.[9]

The purity of the isolated SOMD proteins was assayed by SDS−PAGE (Figure 2). All constructs could be purified as

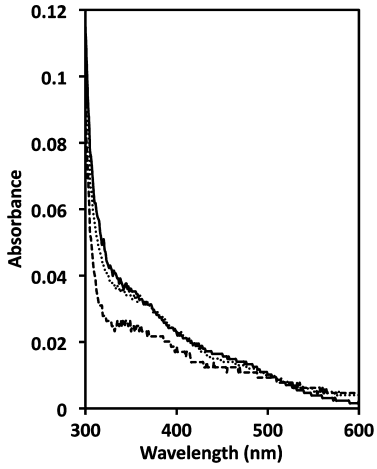

Figure 1. UV−vis absorption spectra of three SOMD constructs: $SOMD_{4Cys(wt)}$ (—), $SOMD_{4Ser}$ (···), and $SeSOMD_{4Ser}$ (---) (5.5 μM). Spectra were recorded in 100 mM Tris (pH 7.2).

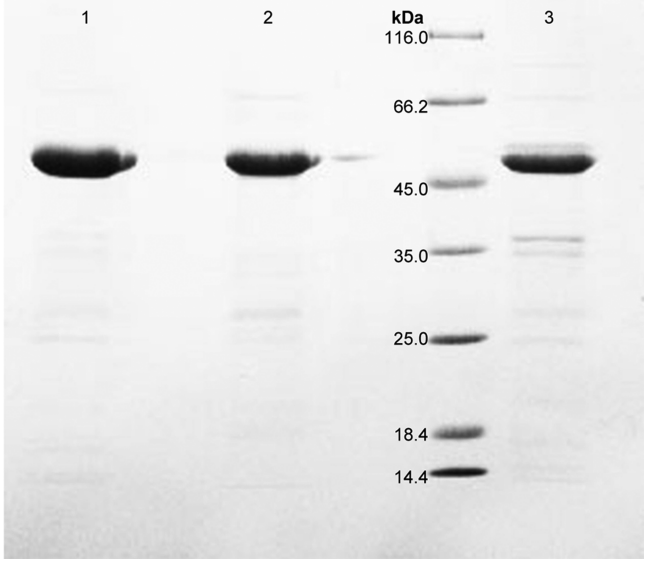

Figure 2. Purity of SOMD proteins. SDS−PAGE (10%) analysis of (1) wild-type $SOMD_{4Cys(wt)}$, (2) $SOMD_{4Ser}$, and (3) $SeSOMD_{4Ser}$ after purification by Ni-NTA chromatography. Each lane contained 12.6 μg of protein.

dimers with a yield of ∼25 mg/L of culture in LB medium and ∼6 mg/L in M9 minimal medium and a purity of ∼95%. ICP-OES revealed a comparable molybdenum content of almost 0.7 Mo ions per SOMD monomer for the constructs after expression in LB medium, and nearly 0.3 Mo ions per $SOMD_{4Ser}$ monomer after expression in the selenocystine-containing minimal medium (data not shown). After heat denaturation of the protein, the Moco-containing supernatant contained only residual amounts of selenium, and the majority of the selenium was identified in the protein fraction, with approximately 0.8 Se per $SOMD_{4Ser}$ monomer. This showed that Sec207 was incorporated into the protein during the expression and not inserted into Moco. Because the cells were first grown on medium containing cysteine as the sulfur source, this would imply that selenocysteine is more rapidly inserted into the protein than into sulfur-containing biomolecules and that for Moco biosynthesis the replacement of sulfur with selenium either is not possible or occurs at a slower rate.

dx.doi.org/10.1021/bi4008512 | Biochemistry 2013, 52, 8295−8303

Steady State Kinetics of SOMD. Steady state activity assays were performed with the three SOMD constructs to determine the kinetic parameters with sulfite as the substrate and ferricyanide as the electron acceptor. The kinetic constants of $SOMD_{4Cys(wt)}$, $SOMD_{4Ser}$, and $SeSOMD_{4Ser}$ are summarized in Table 1. The data show that $SOMD_{4Cys}$ and $SOMD_{4Ser}$ have

Table 1. Enzyme Kinetic Parameters for SOMD Constructs as a Function of pH[a]

pH	k_{cat} (s^{-1})	K_M (μM)	k_{cat}/K_M ($s^{-1}\ \mu M^{-1}$)
$SOMD_{4Cys(wt)}$			
6.0	13.9 ± 0.5	12.1 ± 2.0	1.2 ± 0.2
7.1	16.2 ± 0.6	4.0 ± 0.7	4.1 ± 0.8
7.9	20.8 ± 0.8	4.2 ± 0.8	5.0 ± 1.2
8.4	32.4 ± 1.3	16.6 ± 3.0	2.0 ± 0.4
8.9	27.3 ± 1.0	16.9 ± 2.5	1.6 ± 0.3
$SOMD_{4Ser}$			
6.0	9.4 ± 0.5	9.6 ± 2.5	1.0 ± 0.3
7.1	19.8 ± 1.1	4.8 ± 1.3	4.2 ± 1.4
7.9	19.8 ± 0.8	6.2 ± 1.0	3.2 ± 0.7
8.4	25.8 ± 1.1	10.7 ± 2.9	2.4 ± 0.8
8.9	36.2 ± 2.3	28.8 ± 6.1	1.3 ± 0.4
$SeSOMD_{4Ser}$			
6.0	26.1 ± 1.5	19.0 ± 4.8	1.4 ± 0.4
7.1	46.6 ± 1.8	7.9 ± 1.1	5.9 ± 1.0
7.9	37.7 ± 1.3	8.2 ± 1.2	4.6 ± 0.9
8.4	41.2 ± 1.3	14.6 ± 2.3	2.8 ± 0.5
8.9	31.8 ± 1.4	17.4 ± 3.5	1.8 ± 0.4

[a]Assays were conducted at 25 °C using different buffers, 100 μM ferricyanide, and varying concentrations of sulfite as described in Materials and Methods.

comparable pH profiles for k_{cat} and K_M as reported previously for wild-type SOMD by Wilson and Rajagopalan in 2004,[23] thereby showing that the affinity of sulfite for the enzyme was not largely altered by the four Cys to Ser replacements that were independent of pH. For $SeSOMD_{4Ser}$, k_{cat} and K_M were found to be increased in comparison to those of $SOMD_{4Ser}$, in particular at more neutral pH values. The k_{cat} values of $SOMD_{4Cys(wt)}$ and $SOMD_{4Ser}$ were comparable over the whole pH range (Table 1), showing the highest catalytic activity of 32.4 ± 1.3 s^{-1} at pH 8.4 for $SOMD_{4Cys(wt)}$, as described previously.[23] In contrast, the $SeSOMD_{4Ser}$ construct showed the highest k_{cat} of 46.6 ± 1.8 s^{-1} at pH 7.1, which is 2.3-fold higher than that of the $SOMD_{4Ser}$ construct at the same pH. However, the overall catalytic efficiency was not significantly influenced by the Cys to Sec exchange. The highest catalytic efficiency (5.9 ± 1.0 $s^{-1}\ \mu M^{-1}$) was identified for the $SeSOMD_{4Ser}$ construct at pH 7.1. $SOMD_{4Cys(wt)}$ showed the highest catalytic efficiency of 5.0 ± 1.2 $s^{-1}\ \mu M^{-1}$ at pH 7.9 and the $SOMD_{4Ser}$ construct a value of 3.2 ± 0.7 $s^{-1}\ \mu M^{-1}$ at pH 7.9. Thus, the use of selenocysteine as a ligand to the molybdenum resulted overall in a slight increase in the catalytic efficiency of $SeSOMD_{4Ser}$ by a factor of 1.5, while the pH optimum was shifted more to the neutral region with an optimum at pH 7.1 in the Cys to Ser constructs.

Mo XAS Analysis of the SOMD Constructs. XAS at the Mo K-edge was performed to determine the oxidation state and coordination environment of molybdenum (Figure 3). The XANES spectra of $SOMD_{4Cys(wt)}$, $SOMD_{4Ser}$, and $SeSOMD_{4Ser}$ revealed overall similar spectral shapes and edge energies close to ~20014.5 eV, suggesting a comparable first-sphere

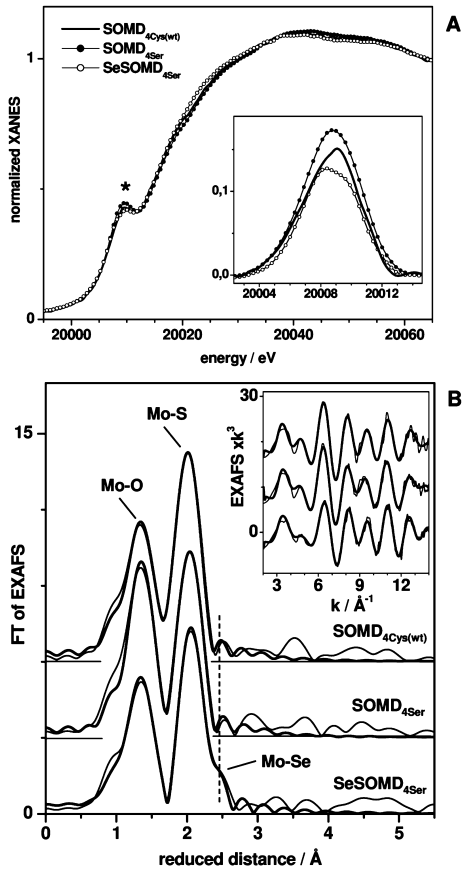

Figure 3. Mo XAS spectra of SOMD constructs at pH 7.1. (A) XANES spectra and isolated pre-edge features (asterisk) in the inset. Edge energies at the 50% level of the XANES (±0.1 eV): $SOMD_{4Cys(wt)}$, 20014.3 eV; $SOMD_{4Ser}$, 20014.6 eV; $SeSOMD_{4Ser}$, 20014.4 eV. (B) Fourier transforms (FTs) of the EXAFS spectra in the inset. Spectra were vertically displaced for comparison. FTs were calculated for k values of 2−14 $Å^{-1}$ using $\cos^2$ windows over 10% of both k range ends. Thin lines show experimental data and thick lines fit curves calculated with the parameters listed in Table 2 (fit numbers 3, 6, and 10). Vertical dashes mark the Mo−Se contribution for $SeSOMD_{4Ser}$.

coordination geometry of the molybdenum ions and a similar oxidation state close to the Mo(VI) level[19] in the three samples (Figure 3A). Compared to that of $SOMD_{4Cys(wt)}$, the pre-edge feature due to 1s → 4d transitions was slightly larger for $SOMD_{4Ser}$ and smaller for $SeSOMD_{4Ser}$, pointing to decreased and increased Mo coordination symmetries in the former and latter proteins.

Simulations of the EXAFS spectra of the three proteins (Figure 3B) provided precise bond lengths at the molybdenum ions (Table 2). The spectrum of $SOMD_{4Cys(wt)}$ was well simulated using approximately two Mo−O and three Mo−S interactions. Tentative splitting of the molybdenum−oxygen shell into two contributions yielded distances of ~1.70 and ~1.75 Å, which presumably suggested the presence of one shorter Mo═O bond and one longer Mo−O^- bond, respectively. Splitting of the sulfur shell yielded two 2.38 Å distances and one 2.48 Å distance. The shorter Mo−S distances likely can be attributed to the sulfurs of the dithiolene group of MPT, and the longer distance can be attributed to the Mo−S(Cys207) interaction. We note, however, that although the fit was improved by the inclusion of two molybdenum−oxygen and molybdenum−sulfur shells, the determined bond length

dx.doi.org/10.1021/bi4008512 | Biochemistry 2013, 52, 8295−8303

Table 2. EXAFS Fit Parameters[a]

		O			S			Se			
	fit	N per Mo	R (Å)	$2\sigma^2 \times 10^3$ (Å^2)	N per Mo	R (Å)	$2\sigma^2 \times 10^3$ (Å^2)	N per Mo	R (Å)	$2\sigma^2 \times 10^3$ (Å^2)	R_F[e] (%)
$SOMD_{4Cys(wt)}$	1	2.05	1.72	8	3.29	2.41	8	–	–	–	8.1
	2	1[b]	1.70	5[c]	2[b]	2.38	2	–	–	–	5.7
		1[b]	1.75	5[c]	1[b]	2.48	1				
	3	1[b]	1.70	3	2[b]	2.38	2	–	–	–	5.2
		0.86[d]	1.76	5[c]	1[b]	2.48	1				
		0.14[d]	1.87	5[c]							
$SOMD_{4Ser}$	4	2.11	1.73	5	3.01	2.42	9	–	–	–	9.1
	5	1[b]	1.71	3[c]	2[b]	2.40	8	–	–	–	7.9
		1[b]	1.73	3[c]	1[b]	2.46	4				
	6	1[b]	1.69	1	2[b]	2.40	7	–	–	–	7.2
		0.96[d]	1.76	2[c]	1[b]	2.47	4				
		0.04[d]	2.01	2[c]							
$SeSOMD_{4Ser}$	7	1.61	1.73	4	2.12	2.41	3	–	–	–	15.6
	8	1.79	1.72	6	2.06	2.41	7	0.91	2.51	9	7.8
	9	1[b]	1.71	5[c]	2[b]	2.41	7	0.67[d]	2.52	7	3.8
		1[b]	1.74	5[c]							
		0.33[d]	2.00	6							
	10	1[b]	1.70	4	2[b]	2.41	7	1[b]	2.51	10	2.9
		0.69[d]	1.77	2[c]							
		0.31[d]	1.99	2[c]							

[a]Definitions: N, coordination number; R, interatomic distance; $2\sigma^2$, Debye–Waller parameter. [b]Indices mark parameters that were fixed in the simulation procedure. [c]Indices mark parameters that were coupled to yield equal values for two shells in the simulation procedure. [d]The sum of two coordination numbers was restrained to unity. [e]The error sum, R_F,[20] was calculated for reduced distances of FTs of 1–2.5 Å.

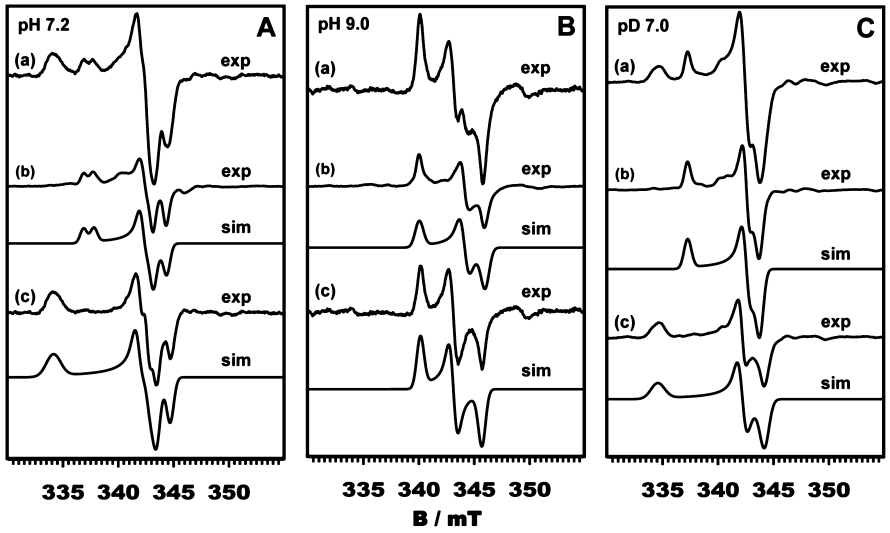

Figure 4. Mo^V EPR spectra of $SOMD_{4Ser}$. (A) Mo^V EPR spectra of various forms of $SeSOMD_{4Ser}$ at pH 7.2. On the basis of the estimated integrated areas, the contribution of the selenated component to the as prepared spectrum is approximately 67%. (B) Mo^V EPR spectra of various forms of $SeSOMD_{4Ser}$ at pH 9.0. (C) Mo^V EPR spectra of various forms of $SeSOMD_{4Ser}$ at pH 6.6 and pD 7.0. (a) Spectrum of partially selenated $SeSOMD_{4Ser}$ as prepared (exp). (b) Sulfurated contribution to the as prepared $SeSOMD_{4Ser}$ spectrum (exp) and its simulation (sim). (c) Selenated contribution to the as prepared $SeSOMD_{4Ser}$ spectrum (exp) obtained by subtraction of spectrum b from spectrum a and its simulation (sim). On the basis of the estimated integrated areas, the contribution of the selenated component to the as prepared spectrum in this sample is approximately 56%. All spectra were aligned to a microwave frequency of 9.4577 GHz.

differences of approximately 0.05–0.10 Å were smaller than the approximate formal distance resolution limit of the EXAFS data (as given by the relation $\Delta R \sim \pi/2\Delta k$) of ~0.13 Å.

The spectrum of $SOMD_{4Ser}$ also was well simulated using two Mo–O and three Mo–S interactions. The smaller Debye–Waller parameter ($2\sigma^2$) of the Mo–O shell in $SOMD_{4Ser}$ (Table 2) explained the increased amplitude of the Mo–O Fourier transform (FT) peak compared to that of $SOMD_{4Cys(wt)}$ (Figure 3B). The similar bond lengths (~1.72 Å) suggested increased contributions from shorter Mo–O bonds in $SOMD_{4Ser}$ compared to those in $SOMD_{4Cys(wt)}$, in agreement with the increased pre-edge feature. This was explained by the overall slightly more oxidized molybdenum in $SOMD_{4Ser}$, as also suggested by the slightly increased K-edge energy (Figure 3A). The Mo–S bonds in $SOMD_{4Ser}$ were similar within ~0.03 Å to those of $SOMD_{4Cys(wt)}$; the two shorter bond lengths (2.40 Å), as derived from a tentative splitting of the Mo–S shell, again were attributed to the MPT ligand, and the longer one

dx.doi.org/10.1021/bi4008512 | Biochemistry 2013, 52, 8295–8303

Table 3. EPR Simulation Parameters for Sulfurated and Selenated Forms of SOMD[a]

		g tensor				A tensor (MHz)			line width ($\times 10^{-3}$)		
		g_1	g_2	g_3	g_{iso}	A_1	A_2	A_3	g_1	g_2	g_3
$SOMD_{4Ser}$	pH 7.2	2.003	1.972	1.966	1.981	26	25	37	4.6	5.2	3.7
$SeSOMD_{4Ser}$		2.022	1.975	1.964	1.987	–	20	35	9.2	4.5	4.3
$SOMD_{4Ser}$	pH 9.0	1.987	1.964	1.953	1.968	–	–	–	4.6	5.2	4.8
$SeSOMD_{4Ser}$		1.987	1.970	1.955	1.970	–	–	–	5.0	4.4	3.8
$SOMD_{4Ser}$	pD 7.0	2.004	1.973	1.966	1.981	–	–	–	5.0	4.2	4.5
$SeSOMD_{4Ser}$		2.020	1.975	1.963	1.986	–	–	–	9.4	5.3	6.2

[a]Proteins at pH 7.2 and 9.0 were dissolved in H_2O, and protein at pD 7.0 was dissolved in D_2O. g_{iso} is the isotropic **g** tensor.

(2.45 Å) was attributed to the Mo−S(Cys) bond. A simulation of the $SeSOMD_{4Ser}$ spectrum using an approach similar to that used for the other two constructs, including two Mo−O and two (Table 2) or three (not shown) Mo−S distances, yielded lower fit qualities compared to the respective fit results for the other two proteins. A largely improved fit quality (R_F diminished by a factor of ∼2) was obtained by the inclusion of an Mo−Se interaction (close to one Mo−Se bond per Mo) with a typical length of ∼2.5 Å[24] (Table 2). The Mo−Se bond manifested as a shoulder on the high-distance side of the Mo−S FT peak (Figure 3B). Calculation of the individual contribution of the Mo−Se bond to the EXAFS spectrum revealed the relatively large amplitudes of the respective FT peak feature and EXAFS oscillations, due to the stronger scattering effect of the heavier Se atom compared to the sulfur atoms (Supporting Information, Figure S1). Replacement of the Mo−Se interaction by a long Mo−S interaction resulted in an ∼2-fold increased R_F value and in an unreasonably small Debye−Waller parameter for the Mo−S bond (data not shown) compared to the parameters for fit 9 in Table 2. In a minor fraction of the protein, the Sec ligand might be replaced by a hydroxo (OH) group (2.00 Å), the inclusion of which significantly improved the fit quality (Table 2). However, attribution of these Mo−OH interactions to the second equatorial ligand appeared to be also a viable option (see below). With respect to the short molybdenum−oxygen interactions (and K-edge energy), $SeSOMD_{4Ser}$ was intermediate between $SOMD_{4Ser}$ and $SOMD_{4Cys(wt)}$. This may point to slightly more reduced molybdenum in $SeSOMD_{4Ser}$, reflecting an increased level of transfer of charge to the Mo from the more covalently bound Se compared to S.

In various molybdoenzymes, protonation equilibria at the Mo site have been observed.[25,26] Inclusion of an additional molybdenum−oxygen interaction in the EXAFS fits, to account for a possible $Mo-O^-$/Mo−OH titration, indeed slightly improved the fit quality for the three proteins (Table 2). The Mo−OH fraction in $SOMD_{4Cys(wt)}$ (∼15%) and in particular in $SeSOMD_{4Ser}$ (∼30%) apparently was larger than in $SOMD_{4Ser}$ (∼5%). The $Mo-O^-$ and Mo−OH bond lengths were determined to be 1.76 and 2.00 Å in both Cys207- and Sec207-containing $SOMD_{4Ser}$ constructs. Notably, an alternative explanation for the presence of small spectral contributions from Mo−OH distances included minor amounts of, for example, Mo(V) centers in the XAS samples.

EPR Analysis of Native and Selenated SOMD. Partially reduced SO is known to exhibit a pH-dependent Mo(V) EPR spectrum.[27] The low-pH spectrum exhibited by $SeSOMD_{4Ser}$ is shown in Figure 4A (spectrum a) and is seen to consist of two specific components. These can be deconvoluted as shown in Figure 4A, with simulations yielding the parameters summarized in Table 1. The minor component in the EPR spectrum obtained at pH 7.2 [Figure 4A (spectrum b)] yields g values that are in full agreement with those of the low-pH signal for wild-type enzyme containing cysteine as a ligand to the molybdenum. Observation of this signal constitutes an internal control that substitution of the four cysteine residues with serine does not significantly perturb the molybdenum center. Simulation of the major component of the EPR signal seen at pH 7.2 yields a **g** tensor with a significantly larger g_1, which we attribute to an enzyme in which Sec has replaced Cys in the molybdenum coordination sphere (Table 3). This assignment is consistent with the known sensitivity of g_1 to the equatorial plane of the molybdenum center, and the expected shift in g_1 to a lower magnetic field (higher g value) upon substitution of Se for S in the molybdenum coordination sphere. Double integration of the two signals indicates that they are present in a 2:1 ratio for Se and S, indicating that approximately 33% of the enzyme in fact possesses cysteine rather than selenocysteine coordinated to the molybdenum. The high-pH EPR signal was also found to be a composite of two components, again in a ratio of 2:1 (Figure 4B). In this case, the g values for the selenated form of the enzyme are much closer to those of the wild-type enzyme, with the most prominent effect being a modest increase in g_2. The smaller effect of substituting selenocysteine for cysteine at high pH as compared to low pH is entirely in keeping with the lower covalency of the Mo−S/Se bonding at high pH compared to that at low pH (increased covalency yielding larger g_1 values[28,29]) upon ionization of the equatorial Mo−OH bond. We find no evidence in the EPR for additional signals that might arise from enzyme forms that might have selenium incorporated into the dithiolene side chain of the cofactor.

The hyperfine coupling seen in the low-pH EPR signal is confirmed to arise from a solvent-exchangeable Mo−OH bond from an examination of samples prepared in D_2O (Figure 4C). Simulations yielded g values essentially identical to those seen in H_2O (Table 1), but the hyperfine coupling has collapsed in both the $SeSOMD_{4Ser}$ and $SOMD_{4Ser}$ signals. Interestingly, the g_1 feature of the $SeSOMD_{4Ser}$ sample remains quite broad, comparable to that seen in the H_2O sample, indicating that the principal contributor to line width broadening on g_1 in the low-pH $SeSOMD_{4Ser}$ signal is related to g strain (even in the H_2O sample).

DISCUSSION

The variable coordination of the metal in molybdenum-containing enzymes is believed to be crucial in modulating the reduction potential and substrate reactivity of the Mo center. In this study, a site-directed mutagenesis approach has been developed and employed to exchange the four non-active site cysteine residues in SOMD of human SO with serine to

dx.doi.org/10.1021/bi4008512 | Biochemistry 2013, 52, 8295−8303

leave only the active site Cys207. This facilitated the specific replacement of Cys207 with a selenocysteine during expression. The Sec207 construct was generated to study the impact of the covalent amino acid ligand on electron transfer and catalytic activity.

The 4Cys → 4Ser exchange preserved the dimeric organization of the SOMD protein, and near-quantitative loading with the cofactor was observed. The change of Cys207 to a selenocysteine so far has not been attempted in SO. Here, selenocystine was added to the expression medium to allow for the incorporation of Sec207 at the active site of the $SOMD_{4Ser}$ construct. The EPR and EXAFS results consistently showed that the Cys207 ligand at the Mo atom was exchanged with Sec. Incorporation of Se into the MPT moiety was not observed, demonstrating that the nonspecific insertion of Sec for Cys occurs first in the protein backbone before Se replaces S in other biomolecules. For Moco biosynthesis, L-cysteine is known to be the primary sulfur donor for the dithiolene moiety of MPT.[30] Sulfur insertion requires an L-cysteine desulfurase in addition to rhodanese-like proteins in a tightly regulated process.[31] However, other S donors also can substitute for cysteine in the cell. For example, in *E. coli*, the sulfur for MPT can be provided by the IscS, TusA, SufS, or YnjE protein *in vivo*,[32] showing that multiple sulfur transfer relay systems exist in the cell. These proteins may act also in S storage during periods of sulfur limitation. Accordingly, a possible reason for the absence of incorporation of Se into MPT in $SOMD_{4Ser}$ protein was that the cells were not starved long enough for sulfur prior to protein expression. Apparently, Sec either could not serve as a Se source or was handled at a much slower rate by the Moco biosynthesis machinery than Cys, facilitating specific analysis of the effects of the Cys207 to Sec replacement at the active site.

Comparable sulfite oxidizing activities in $SOMD_{4Cys(wt)}$ and $SOMD_{4Ser}$ demonstrated that the functionality of the Moco site was fully preserved in the mutant. EPR and XAS analyses also revealed that the structural integrity of the molybdenum center itself remained intact, both in its Mo(V) and Mo(VI) oxidation states and for a wide pH range. The $SOMD_{4Ser}$ system thus represents a viable platform for studying the substitution of the Cys207 ligand with Sec. The XAS and EPR data indicated that Se is bound to Mo(V) and Mo(VI) in $SeSOMD_{4Ser}$. However, the relatively large EXAFS Debye–Waller parameter of the molybdenum–selenium interaction suggested a distance spread of ±0.07 Å corresponding to Mo(VI)–Se bond lengths in the range of at least 2.44–2.58 Å and thus considerable disorder in Mo–Se bonding. The considerable degree of *g* strain, manifested in the broad line width of the g_1 feature of the Mo(V) EPR signal, also implied heterogeneity in the Mo coordination of Sec207. Presumably, these results are explained by varying bonding angles and Mo–Se distances due to a more flexible configuration of the Sec207 side chain compared to that of Cys207.

The sulfite oxidizing activity of $SeSOMD_{4Ser}$ was increased by a mean factor of ∼1.5 over that of $SOMD_{4Ser}$, which in turn was similar to that of $SOMD_{4Cys(wt)}$, indicating that all three constructs were fully functional in catalysis. However, taking into account the fact that only approximately two-thirds of the protein possesses Sec207, we found the increase in catalytic efficiency might be corrected to a factor of ∼1.67 in the fully Sec-substituted protein. Also, the determined K_M values were comparable to those of a previous report for human $SOMD_{4Cys(wt)}$.[23] In contrast, replacement of Cys207 in SO with a serine ligand resulted in the loss of catalytic activity.[9,10] A distance of 3.6 Å between the Mo and the hydroxyl oxygen of the Ser side chain precluded direct ligation of Ser at the Mo center, and instead, a third oxo/hydroxo ligand was bound to the Mo.[10,25] The loss of catalytic activity thus could be explained by the perturbation of both the Mo^{VI}/Mo^{V} and Mo^{V}/Mo^{IV} redox potentials by oxygen binding, even when the square pyramidal geometry of the Mo center was preserved. Selenium and sulfur are substantially less electronegative than oxygen [Pearson electronegativities (5.89 eV for Se < 6.22 eV for S < 7.54 eV for O)]. The increasing activities of SO for ligand exchange at the Mo in the order Se > S > O suggest that the more covalent character of the metal–ligand bond for Se and S compared to O is a major factor in the modulation of enzyme activity.

Our studies support previous suggestions that the primary role of the coordinated cysteine is to decrease the effective charge on the molybdenum by donation of electron density to the metal, contributing to more negative reduction potentials at the active site during electron transfer to cytb_5.[33] Upon replacement of Cys207 with Ser, the covalent molybdenum bond is not formed. Instead, replacement with Sec preserves the covalency of the bond and thus the catalytic activity of the enzyme. Because the more covalent bond is not thought to contribute in the catalytic mechanism during sulfite oxidation,[34] the kinetic constants in the Sec207 construct are only slightly increased. Similar results were obtained in studies of azurin, in which the Cu–S and Cu–Se bonding effects were compared.[35] These studies showed that the $Cu–S_{Cys}$ and $Cu–Se_{Cys}$ bonds have similar covalencies and lengths, which supports our observation that Cys207 can be replaced with Sec in SO. In contrast, the situation seen in the Sec-containing formate dehydrogenases is different, where the Sec residue is directly involved in substrate turnover and has been proposed to act as a proton acceptor during catalysis.[36] Thus, replacement of the naturally occurring Sec with Cys in *E. coli* FdhF resulted in a decrease in catalytic activity by a factor of 300 from 2800 to 9 s^{-1}.[37] In this case, the difference in the p*K* values of Cys (8.2) and Sec (5.2) is more important for the reaction, because for protonation during the reaction of FdhF, Sec needs to be in a deprotonated state. Thus, in FdhF, the presence of Cys instead of Sec does not tune the redox reactivity of the metal center; instead, the pK_a of the selenolate is required for efficient catalysis.

■ ASSOCIATED CONTENT

Supporting Information

Mo-Se contribution to the EXAFS (Figure S1). This material is available free of charge via the Internet at http://pubs.acs.org.

■ AUTHOR INFORMATION

Corresponding Author

*Institut für Biochemie and Biologie, Molekulare Enzymologie, Universität Potsdam, Karl-Liebknecht-Str. 24-25, 14476 Potsdam, Germany. E-mail: sleim@uni-potsdam.de. Phone: +49-331-977-5603. Fax: +49-331-977-5128.

Present Address

⊥MAX IV Laboratory, Lund University, 22100 Lund, Sweden.

Funding

This work was supported by the Deutsche Forschungsgemeinschaft (DFG) Cluster of Excellence "Unifying Concepts in Catalysis" (EXC 314), by DFG Grant LE1171/6-1 (to S.L.),

and by a Heisenberg Fellowship and Grants Ha3265/3-1 and Ha3265/6-1 from the DFG (to M.H.). K.G.V.S. thanks "Stiftelsen Bengt Lundqvist minne" and the Wenner-Gren Foundation for fellowships. R.H. is grateful for grant support from the U.S. Department of Energy.

Notes

The authors declare no competing financial interest.

■ ABBREVIATIONS

EPR, electron paramagnetic resonance spectroscopy; EXAFS, extended X-ray absorption fine structure; Moco, molybdenum cofactor; MPT, molybdopterin; SO, sulfite oxidase; SOMD, sulfite oxidase Moco binding domain; XANES, X-ray absorption near-edge structure; XAS, X-ray absorption spectroscopy.

■ REFERENCES

(1) Kisker, C., Schindelin, H., and Rees, D. C. (1997) Molybdenum-cofactor-containing enzymes: Structure and mechanism. *Annu. Rev. Biochem. 66*, 233−267.

(2) Hille, R. (1996) The mononuclear molybdenum enzymes. *Chem. Rev. 96*, 2757−2816.

(3) Kisker, C., Schindelin, H., Pacheco, A., Wehbi, W. A., Garrett, R. M., Rajagopalan, K. V., Enemark, J. H., and Rees, D. C. (1997) Molecular basis of sulfite oxidase deficiency from the structure of sulfite oxidase. *Cell 91*, 973−983.

(4) Johnson, J. L., Hainline, B. E., and Rajagopalan, K. V. (1980) Characterization of the molybdenum cofactor of sulfite oxidase, xanthine oxidase and nitrate reductase. Identification of a pteridine as a structural component. *J. Biol. Chem. 255*, 1783−1786.

(5) Johnson, J. L., Waud, W. R., Rajagopalan, K. V., Duran, M., Beemer, F. A., and Wadman, S. K. (1980) Inborn errors of molybdenum metabolism: Combined deficiencies of sulfite oxidase and xanthine dehydrogenase in a patient lacking the molybdenum cofactor. *Proc. Natl. Acad. Sci. U.S.A. 77*, 3715−3719.

(6) Brody, M. S., and Hille, R. (1999) The kinetic behavior of chicken liver sulfite oxidase. *Biochemistry 38*, 6668−6677.

(7) Feng, C., Kedia, R. V., Hazzard, J. T., Hurley, J. K., Tollin, G., and Enemark, J. H. (2002) Effect of solution viscosity on intramolecular electron transfer in sulfite oxidase. *Biochemistry 41*, 5816−5821.

(8) Temple, C. A., and Rajagopalan, K. V. (2000) Optimization of Expression of Human Sulfite Oxidase and its Molybdenum Domain. *Arch. Biochem. Biophys. 383*, 281−287.

(9) Garrett, R. M., and Rajagopalan, K. V. (1996) Site-directed mutagenesis of recombinant sulfite oxidase. Identification of cysteine 207 as a ligand of molybdenum. *J. Biol. Chem. 271*, 7387−7391.

(10) George, G. N., Garrett, R. M., Prince, R. C., and Rajagopalan, K. V. (2004) Coordination chemistry at the molybdenum site of sulfite oxidase: Redox-induced structural changes in the cysteine 207 to serine mutant. *Inorg. Chem. 43*, 8456−8460.

(11) Karakas, E., Wilson, H. L., Graf, T. N., Xiang, S., Jaramillo-Busquets, S., Rajagopalan, K. V., and Kisker, C. (2005) Structural insights into sulfite oxidase deficiency. *J. Biol. Chem. 280*, 33506−33515.

(12) Wessjohann, L. A., Schneider, A., Abbas, M., and Brandt, W. (2007) Selenium in chemistry and biochemistry in comparison to sulfur. *Biol. Chem. 388*, 997−1006.

(13) Jormakka, M., Byrne, B., and Iwata, S. (2003) Formate dehydrogenase: A versatile enzyme in changing environments. *Curr. Opin. Struct. Biol. 13*, 418−423.

(14) Wagener, N., Pierik, A. J., Ibdah, A., Hille, R., and Dobbek, H. (2009) The Mo-Se active site of nicotinate dehydrogenase. *Proc. Natl. Acad. Sci. U.S.A. 106*, 11055−11060.

(15) Gladyshev, V. N., Khangulov, S. V., Axley, M. J., and Stadtman, T. C. (1994) Coordination of selenium to molybdenum in formate dehydrogenase H from *Escherichia coli*. *Proc. Natl. Acad. Sci. U.S.A. 91*, 7708−7711.

(16) Müller, S., Heider, J., and Böck, A. (1997) The path of unspecific incorporation of selenium in *Escherichia coli*. *Arch. Microbiol. 168*, 421−427.

(17) Laemmli, U. K. (1970) Cleavage of structural proteins during the assembly of the head of bacteriophage T4. *Nature 227*, 680−685.

(18) Neumann, M., and Leimkühler, S. (2008) Heavy metal ions inhibit molybdoenzyme activity by binding to the dithiolene moiety of molybdopterin in *Escherichia coli*. *FEBS J. 275*, 5678−5689.

(19) Havelius, K. G., Reschke, S., Horn, S., Doring, A., Niks, D., Hille, R., Schulzke, C., Leimkühler, S., and Haumann, M. (2011) Structure of the molybdenum site in YedY, a sulfite oxidase homologue from *Escherichia coli*. *Inorg. Chem. 50*, 741−748.

(20) Dau, H., Liebisch, P., and Haumann, M. (2003) X-ray absorption spectroscopy to analyze nuclear geometry and electronic structure of biological metal centers: Potential and questions examined with special focus on the tetra-nuclear manganese complex of oxygenic photosynthesis. *Anal. Bioanal. Chem. 376*, 562−583.

(21) Zabinsky, S. I., Rehr, J. J., Ankudinov, A., Albers, R. C., and Eller, M. J. (1995) Multiple-scattering calculations of X-ray-absorption spectra. *Phys. Rev. B: Condens. Matter Mater. Phys. 52*, 2995−3009.

(22) Stoll, S., and Schweiger, A. (2006) EasySpin, a comprehensive software package for spectral simulation and analysis in EPR. *J. Magn. Reson. 178*, 42−55.

(23) Wilson, H. L., and Rajagopalan, K. V. (2004) The role of tyrosine 343 in substrate binding and catalysis by human sulfite oxidase. *J. Biol. Chem. 279*, 15105−15113.

(24) Musgrave, K. B., Lim, B. S., Sung, K. M., Holm, R. H., Hedman, B., and Hodgson, K. O. (2000) X-ray spectroscopy of enzyme active site analogues and related molecules: Bis(dithiolene)molybdenum(IV) and -tungsten(IV,VI) complexes with variant terminal ligands. *Inorg. Chem. 39*, 5238−5247.

(25) George, G. N., Garrett, R. M., Prince, R. C., and Rajagopalan, K. V. (1996) The molybdenum site of sulfite oxidase: A comparison of the wild-type and the cysteine 207 to serine mutant using X-ray absorption spectroscopy. *J. Am. Chem. Soc. 118*, 8588−8592.

(26) George, G. N., Kipke, C. A., Prince, R. C., Sunde, R. A., Enemark, J. H., and Cramer, S. P. (1989) Structure of the active site of sulfite oxidase. X-ray absorption spectroscopy of the Mo(IV), Mo(V), and Mo(VI) oxidation states. *Biochemistry 28*, 5075−5080.

(27) Klein, E. L., Astashkin, A. V., Raitsimring, A. M., and Enemark, J. H. (2013) Applications of pulsed EPR spectroscopy to structural studies of sulfite oxidizing enzymes. *Coord. Chem. Rev. 257*, 110−118.

(28) Yang, J., Rothery, R., Sempombe, J., Weiner, J. H., and Kirk, M. L. (2009) Spectroscopic characterization of YedY: The role of sulfur coordination in a Mo(V) sulfite oxidase family enzyme form. *J. Am. Chem. Soc. 131*, 15612−15614.

(29) Peariso, K., Chohan, B. S., Carrano, C. J., and Kirk, M. L. (2003) Synthesis and EPR characterization of new models for the one-electron reduced molybdenum site of sulfite oxidase. *Inorg. Chem. 42*, 6194−6203.

(30) Leimkühler, S., and Rajagopalan, K. V. (2001) A sulfurtransferase is required in the transfer of cysteine sulfur in the in vitro synthesis of molybdopterin from precursor Z in *Escherichia coli*. *J. Biol. Chem. 276*, 22024−22031.

(31) Dahl, J. U., Urban, A., Bolte, A., Sriyabhaya, P., Donahue, J. L., Nimtz, M., Larson, T. J., and Leimkühler, S. (2011) The identification of a novel protein involved in molybdenum cofactor biosynthesis in *Escherichia coli*. *J. Biol. Chem. 286*, 35801−35812.

(32) Dahl, J. U., Radon, C., Bühning, M., Nimtz, M., Leichert, L. I., Denis, Y., Jourlin-Castelli, C., Iobbi-Nivol, C., Mejean, V., and Leimkühler, S. (2013) The Sulfur Carrier Protein TusA Has a Pleiotropic Role in *Escherichia coli* That Also Affects Molybdenum Cofactor Biosynthesis. *J. Biol. Chem. 288*, 5426−5442.

(33) Helton, M. E., Pacheco, A., McMaster, J., Enemark, J. H., and Kirk, M. L. (2000) An MCD spectroscopic study of the molybdenum active site in sulfite oxidase: Insight into the role of coordinated cysteine. *J. Inorg. Biochem. 80*, 227−233.

(34) Peariso, K., Helton, M. E., Duesler, E. N., Shadle, S. E., and Kirk, M. L. (2007) Sulfur K-edge spectroscopic investigation of second

coordination sphere effects in oxomolybdenum-thiolates: Relationship to molybdenum-cysteine covalency and electron transfer in sulfite oxidase. *Inorg. Chem. 46*, 1259−1267.
(35) Sarangi, R., Gorelsky, S. I., Basumallick, L., Hwang, H. J., Pratt, R. C., Stack, T. D., Lu, Y., Hodgson, K. O., Hedman, B., and Solomon, E. I. (2008) Spectroscopic and density functional theory studies of the blue-copper site in M121SeM and C112SeC azurin: Cu-Se versus Cu-S bonding. *J. Am. Chem. Soc. 130*, 3866−3877.
(36) Mota, C. S., Rivas, M. G., Brondino, C. D., Moura, I., Moura, J. J., Gonzalez, P. J., and Cerqueira, N. M. (2011) The mechanism of formate oxidation by metal-dependent formate dehydrogenases. *JBIC, J. Biol. Inorg. Chem. 16*, 1255−1268.
(37) Axley, M. J., Bock, A., and Stadtman, T. C. (1991) Catalytic properties of an *Escherichia coli* formate dehydrogenase mutant in which sulfur replaces selenium. *Proc. Natl. Acad. Sci. U.S.A. 88*, 8450−8454.